

Herbig-Haro flows around BBWo 192E (GM 1-23) nebula

T.Yu. Magakian^{1*}, T.A. Movsessian¹, H.R. Andreasyan¹, J.Bally² and A.S. Rastorguev^{3,4}

¹*Byurakan Observatory of the Nat.Acad.Sci. of Armenia, Byurakan, Aragatsotn prov., 0213, Armenia*

²*Department of Astrophysical and Planetary Sciences, University of Colorado, Boulder, CO, USA*

³*Faculty of Physics, Lomonosov Moscow State University, Leninskie Gory 1, bldg.2, Moscow, Russia*

⁴*Sternberg Astronomical Institute, Lomonosov Moscow State University, Universitetskii prospect 13, Moscow, Russia*

ABSTRACT

We studied a small comet-shape reflection nebula, located in the dark cloud SL 4 in the Vela Molecular Ridge cloud C, known as BBWo 192E (GM 1-23), and a young infrared cluster embedded into the nebula, for the evidences of recent star formation. We obtained the images of BBWo 192E in H α and [S II] lines and in SDSS i' with Blanco telescope at the Cerro Tololo Interamerican Observatory to discover new Herbig-Haro (HH) flows. 2MASS and WISE surveys were used for the search of the additional member stars of the cluster. We also studied proper motions and parallaxes of the cluster members with the aid of GAIA DR2. Five new groups containing at least 9 HH objects tracing several distinct outflows were revealed. A previously unreported reflection nebula and a number of probable outflow sources were found in the infrared range. The proper motions allowed selecting eight probable member stars in the visual range. Their parallaxes correspond to a mean distance 800 ± 100 pc for this cluster. The bolometric luminosities of the brightest cluster members are $1010 L_{\odot}$ (IRAS 08513–4201, the strong source in the center of the cluster) and 2 to 6 L_{\odot} for the five other stars. The existence of the optical HH flows around the infrared cluster of YSOs suggests that star formation in this cloud is on-going around the more massive HAeBe star. By its morphology and other features this star-forming region is similar to the zone of star formation near CPM 19.

Key words: open clusters and associations; stars: pre-main-sequence; ISM: jets and outflows, Herbig-Haro objects

1 INTRODUCTION

A small comet-shape reflection nebula, located in the elongated dark cloud SL 4 (Sandqvist & Lindroos 1976) in the Vela Molecular Ridge cloud C (Murphy & May 1991), is known as GM 1-23 (Gyulbudaghian & Magakian 1977) and BBWo 192E (Brand, Blitz & Wouterloot 1986). Such nebulous objects are often indicators of ongoing star formation and this case is no exception. The survey of Petterson & Reipurth (1994) revealed tens of H α emission-line stars in the vicinity of SL 4, but did not find any Herbig-Haro (HH) objects. The BBWo 192E nebula was studied for the first time in this work; the authors concluded that it was a reflection nebula and that the relatively bright star on its northern edge is a projected foreground object. They suggested that the illuminating star is embedded in the cloud and should be HAeBe type young star.

This BBWo 192E nebula is associated with a bright and very red source, IRAS 08513–4201, recognized as a

Class I object with a near-IR counterpart (Liseau et al. 1992). Further multi-frequency studies (Burkert et al. 2000; Massi, Lorenzetti & Giannini 2003; Dutra et al. 2003) in the near and mid-infrared revealed a young infrared cluster embedded in the nebula. IRAS 08513–4201 was found to be its most luminous member, illuminating not only the optical nebula but also a bipolar IR reflection nebula. The distance of this group was estimated by Burkert et al. (2000) ~ 1.2 kpc. These findings led us to search for HH objects and collimated outflows in the BBWo 192E field with narrow-band filters.

2 OBSERVATIONS AND DATA REDUCTION

The images presented here were obtained on the nights of 13 May 2004 using the NOAO Mosaic II Camera CCD camera at the f/3.1 prime focus of the 4 meter Blanco telescope at the Cerro Tololo Interamerican Observatory (CTIO) near La Serena, Chile. Mosaic II camera is a 8192×8192 pixel array (consisting of eight 2048×4096 pixel CCD chips) with

* E-mail: tigmag@sci.am

Table 1. List of the new HH objects

Knot	α (J2000)	δ (J2000)
	h m s	° ' "
HH 1204	08 53 08.1	-42 12 10
HH 1205C	08 53 02.8	-42 13 14
HH 1205B	08 58 07.0	-42 12 49
HH 1205A	08 53 09.5	-42 12 34
HH 1206	08 53 10.9	-42 14 13
HH 1207A	08 53 14.0	-42 14 10
HH 1207B	08 53 12.7	-42 14 07
HH 1208A	08 53 13.1	-42 14 34
HH 1208B	08 53 12.9	-42 14 41

a pixel scale of $0.26'' \text{ pixel}^{-1}$ and a field of view $35.4'$ on a side.

Narrow-band filters centered on 6569\AA and 6730\AA with a FWHM bandwidth of 80\AA were used to obtain $H\alpha$ and $[S\ II]$ images. A Sloan Digital Sky Survey (SDSS) i' filter centered on 7732\AA with a FWHM of 1548\AA was used for continuum imaging. A set of five dithered 600 second exposures were obtained in $H\alpha$ and $[S\ II]$ using the standard MOSDITHER pattern to eliminate cosmic rays and the gaps between the individual chips in Mosaic. A dithered set of five 180 second exposures were obtained in the broad-band SDSS i -band filter to discriminate between $H\alpha$, $[S\ II]$, and continuum emission.

Images were reduced in the standard manner using IRAF. Following bias subtraction, cosmic ray removal, and flat fielding using dome flats, images were combined using the MSCRED package in IRAF. Due to insufficient observational time over the whole images there are remaining parts with low S/N.

3 RESULTS

3.1 Visual wavelength imaging

The images reveal several small shock-excited emission nebulae in two or three groups seen in the $H\alpha$ and $[S\ II]$ narrow-band filters but not in the broad i' -band filter. Given their morphology, they are likely to be HH objects which are too faint to have been seen in the previous searches. Their coordinates are given in Table 1 and images are shown on Fig. 1 and Fig. 2. Fig. 3, where they can be seen better, shows the subtraction of a scaled version of the i' -band image from the $[S\ II]$ image, with the intensity adjusted so that stars have similar counts in the i' and $[S\ II]$ images. The brightest part of BBWo 192E nebula also remains visible in this figure, which may indicate the presence of reflected emission from the central source. We checked the DECaPS survey (Schlafly et al. 2018) in which these HH objects are also detected. However, they cannot be distinguished by color from the other red stars and nebulous wisps.

As seen in Figs. 1 – 3, all HH knots are brighter in $[S\ II]$ emission. One group of HH objects is located near the northern side of reflection nebula. Two elongated streaks superimposed on the BBWo 192E nebula, labeled as knots A and

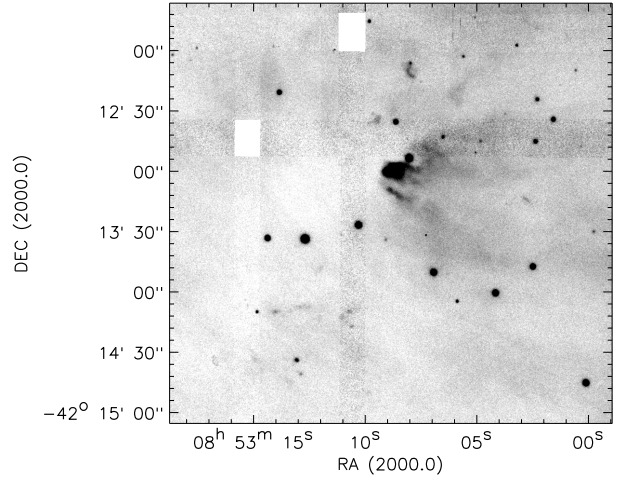


Figure 1. BBWo 192E nebula and new HH objects around it in $[S\ II]$ filter. Rectangular artifacts are produced during the image processing.

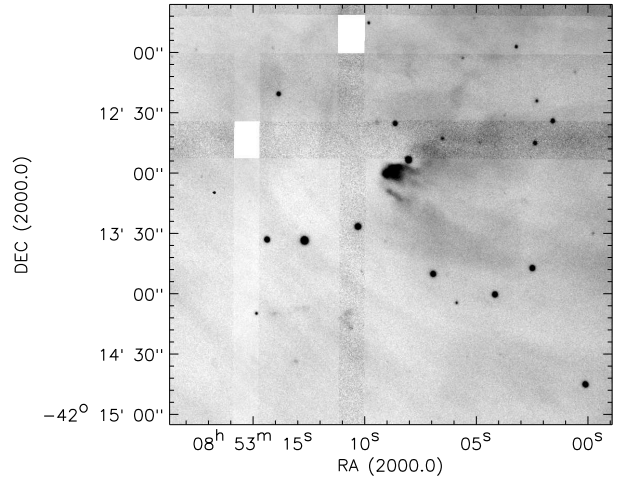


Figure 2. Same field in $H\alpha$ filter.

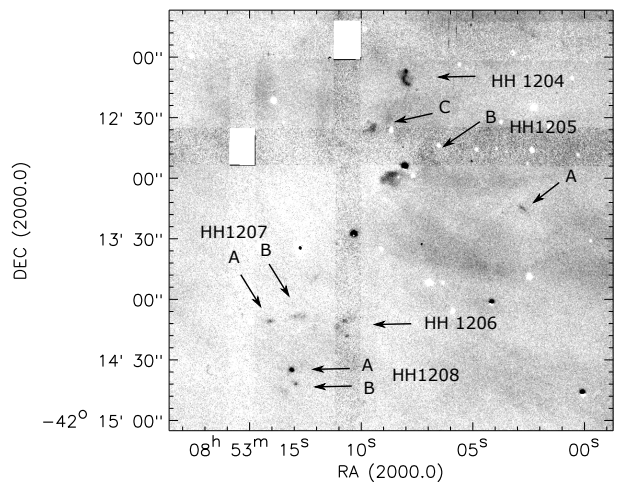


Figure 3. Same field in $[S\ II]$ filter after continuum subtraction. HH objects are marked by arrows.

B in Fig. 3, along with knot C located north of the reflection nebula core, form the chain we call HH 1205. The three components, HH 1205 A, B and C, form a nearly straight line and therefore probably trace shocks in one outflow with a full extent of about $85''$, corresponding to a projected length about a half of parsec at the assumed distance to this complex. To be sure that the streak HH 1205 B is a real emission structure and not a remnant of continuum subtraction, we want to note that it is invisible in $H\alpha$ image and, on the other hand, the brighter nebulous structure, located to the south from it, is completely subtracted in Fig. 3.

HH 1204 is an arcuate feature located about $30''$ north of the HH 1205 chain, practically visible only in [S II].

A second group of HH objects, HH 1206, HH 1207, and HH 1208, located about 90 to $120''$ southeast of BBWo 192E. HH 1206, resembles a bow-shock containing several small knots. HH 1207 consists of two streaks elongate east-to-west and may trace parts of a collimated flow. HH 1208 comprises two nearly-stellar knots. They are projected on several faint, nebulous wisps which may be reflection nebulae, given their visibility in the i' image.

Thus, the BBWo 192E field contains at least 9 HH objects tracing several distinct outflows. However, none are associated with visual wavelength stars that are likely driving sources. The stars that drive these outflows are more likely to be highly obscured. The observed HH objects may trace material ejected from the cloud into the relatively extinction-free foreground.

3.2 Infrared data

We searched the literature for near-IR studies and inspected several public-domain data sets such as 2MASS and WISE to search for the probable driving sources these HH objects. Dutra et al. (2003) found a small infrared cluster (#22 in their list) associated with BBWo 192E, the existence of which was also suspected in the study of Burkert et al. (2000). This cluster includes also a small nebula, which is the IR analog of BBWo 192E, and is seen in the 2MASS survey (Fig. 4). Star #28 from the work of Burkert et al. (2000), visible only at IR wavelengths, coincides with the straight line connecting HH 1205 A, B and C. As is discussed in the same paper, star #28 is likely to be a pre-main-sequence (PMS) star inside the cloud. It has very red colors according to Massi, Lorenzetti & Giannini (2003, star IRS 26-35) and is a likely candidate source powering the HH 1205 outflow. There are no infrared sources near HH 1204.

The near-IR (J, H, K-band) 2MASS images reveal another small, near-IR reflection nebula $\sim 2'$ to southeast of BBWo 192E in the vicinity of the southeastern group of HH objects (see Fig. 4; J2000.0 coordinates, RA = $8^h 53^m 15^s$, Dec = $-42^\circ 14' 31''$). This nebula is not seen in the visual wavelength images and was not previously mentioned in any catalogs or surveys. The 2MASS Point Source Catalog lists seven sources inside the nebula, at least some of which may be embedded young stars. Thus, the existence of a compact infrared cluster of PMS stars inside this nebula seems probable. HH 1206 and HH 1207 are located northwest of this wedge-shaped IR reflection nebula; HH 1206 is close to its axis of symmetry. However, it is unclear which, if any of the IR sources, visible in this region, powers HH 1206, 1207, and 1208.

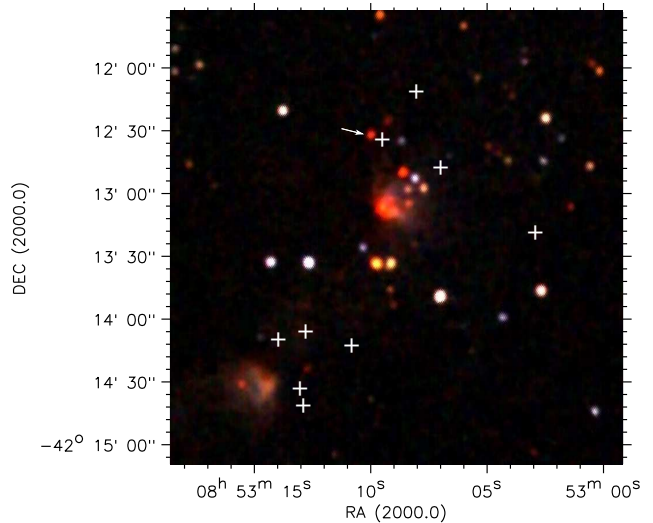


Figure 4. Color representation of the investigated field from 2MASS survey (J - blue, H - green, K - red). Two infrared nebulae are prominent. The positions of HH objects are marked by white crosses. Star #28 a.k.a. IRS 26-35 (Burkert et al. 2000; Massi, Lorenzetti & Giannini 2003) is pointed by arrow.

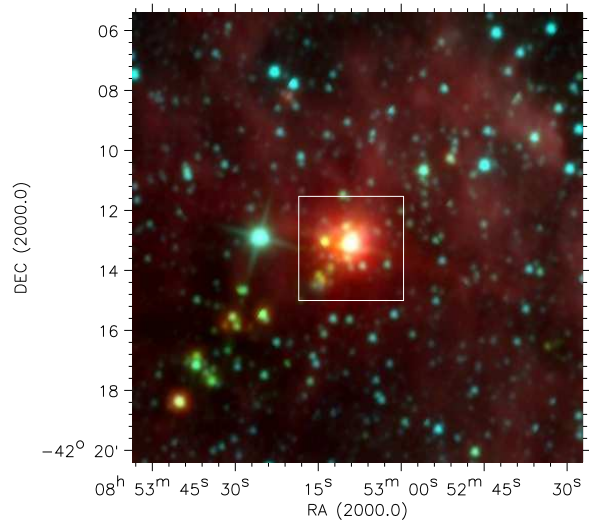


Figure 5. Color image of a wide field around BBWo 192E from WISE survey (blue - $3.3 \mu\text{m}$, green - $4.7 \mu\text{m}$, red - $22 \mu\text{m}$). The area, presented in Figs 1 – 4, is shown by white square.

The clustering of embedded sources around BBWo 192E is apparent in the longer mid-IR WISE survey ($\lambda = 3.3, 4.7, 12, \text{ and } 22 \mu\text{m}$; Wright et al. 2010) (Fig. 5). Wider field-of-view images reveal several additional infrared sources in the region. IRAS 08513–4201, located near the apex of the BBWo 192E nebula, dominates the field. Many additional sources not seen in the 2MASS images are also visible. The most prominent objects are marked in Fig. 6 and described below. Their designations are those of the allWISE source catalog along with the numbers from the list of J, H, and K photometry by Massi, Lorenzetti & Giannini (2003).

J085309.91-421232.6 (IRS 26-35). This source was discussed above. The WISE data confirm its large mid-IR

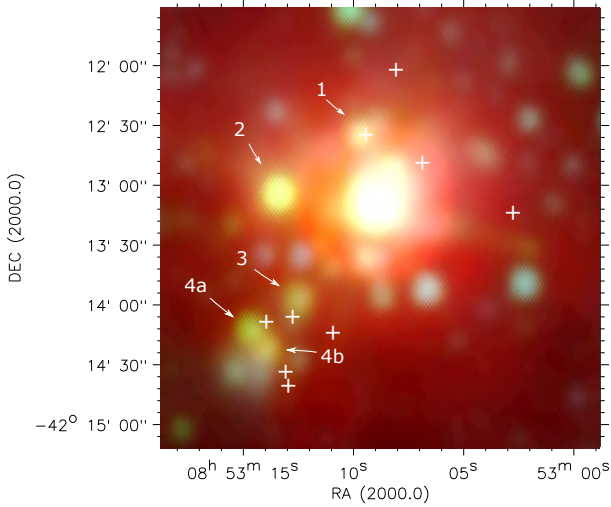


Figure 6. The central part of the WISE field shown in Fig.5. The bright object in the center is IRAS 08513-4201. The positions of HH objects are marked by white crosses. The sources, described in text, are marked by numbers: 1) - J085309.91-421232.6; 2) - J085313.68–421301.6; 3) - J085312.79-421355.2; 4a,b) - J085314.89-421411.4 and J085314.29-421420.2.

brightness which peaks at $22\ \mu\text{m}$ (no longer-wavelength photometric data can be found), making it likely to be a young stellar objects (YSO). It may be the source of the HH 1205 outflow.

J085313.68-421301.6 (IRS 26-19). This source, located $48''$ east from IRAS 08513-4201, is absent at all 2MASS wavelengths but visible in the WISE $3.3\ \mu\text{m}$ image. It becomes prominent at longer wavelengths, second only to IRAS 08513-4201. It illuminates the cone-shaped IR reflection nebula, oriented northward. It is invisible in the 2MASS K-band and in the K-band image in Burkert et al. (2000). However, it appears near the limit ($K = 16.85$) in the image presented by Massi, Lorenzetti & Giannini (2003) which makes it one of the reddest objects in the field.

J085312.79-421355.2 (IRS 26-52). This object located between two IR reflection nebulae described above is absent in the 2MASS catalog, but according to Massi, Lorenzetti & Giannini (2003) is brighter ($K = 15.39$) than the previous object. On WISE images it appears embedded in the faint nebula. However, it is not as red as J085313.68–421301.6.

J085314.89-421411.4 and J085314.29-421420.2. This is a pair of the sources on the north-western side of the newly described IR reflection nebula. They are located outside of the area, studied by Massi, Lorenzetti & Giannini (2003). The eastern source is brighter in near IR and can be found in the 2MASS all-sky PSC; the western source becomes brighter at $12\ \mu\text{m}$ in the WISE image. These sources may be the main illuminators of the reflection nebula. They are candidate drivers of the outflows containing HH 1207 and HH 1208.

3.3 Proper motions and distance

Most stars in the IR cluster inside BBWo 192E are invisible in the visual wavelength range. Nevertheless, new astromet-

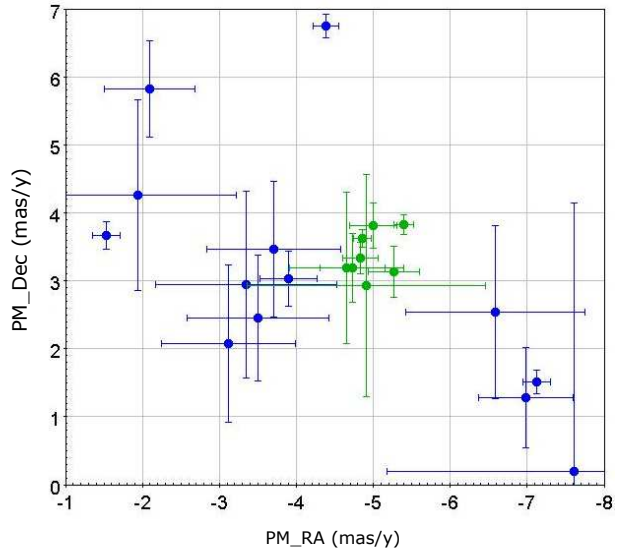


Figure 7. The diagram of proper motions and their error bars for the stars in BBWo 192E field. The stars with most similar PM are marked by green color.

ric data from the GAIA DR2 catalog allow a search for additional members of this cluster which are not too embedded.

We studied the field around IRAS 08513-4201 within a $3'$ radius. The GAIA DR2 catalog contains 61 stars. From these we selected stars with parallaxes in the $0.7\text{--}1.8\ \text{mas}$ range, taking into account the systematic correction $+0.045\ \text{mas}$ (see, e.g. Schönrich, McMillan & Eyer 2019). The exact value of this correction is not significant at the distances less than $1\ \text{kpc}$.

Fig. 7 shows the distribution of their proper motions (PM) in right ascension and declination. There are 8 stars with similar proper-motion values. These stars have similar parallaxes (see Fig. 8) with a mean value of $1.32 \pm 0.18\ \text{mas}$ corresponding to a mean distance $800 \pm 100\ \text{pc}$. Their mean PM is $-4.89 \pm 0.19\ \text{mas/y}$ (RA) and $+3.17 \pm 0.28\ \text{mas/y}$ (Dec). One more argument for the possible relationship between this group of stars and the IR cluster is their very red colors (BP–RP values are in $2.5\text{--}3.7$ range).

There are 6 additional faint stars with G magnitude in the $18.5\text{--}20.2$ range whose PMs are similar to the 8 brighter stars, but their parallax and proper-motion errors are large. Thus, these stars may also be members of the cluster. However, they are located at greater projected distance from the center of the cluster than the eight selected stars.

We show the positions of eight probable member stars in Fig. 9. For completeness, in Table 2 we list their positions and distances according to the catalogue of Bailer-Jones et al. (2018). These distances are estimated by the Bayes method, taking into account selection effects. The mean distance, computed by these data, is $940\ \text{pc}$. The difference in values can be explained by various corrections for the systematic error in parallaxes.

Six of these stars have IR photometry in Burkert et al. (2000), three – in Massi, Lorenzetti & Giannini (2003). One of these stars is an emission-line star, ESO-H α 259 (Pettersson & Reipurth 1994).

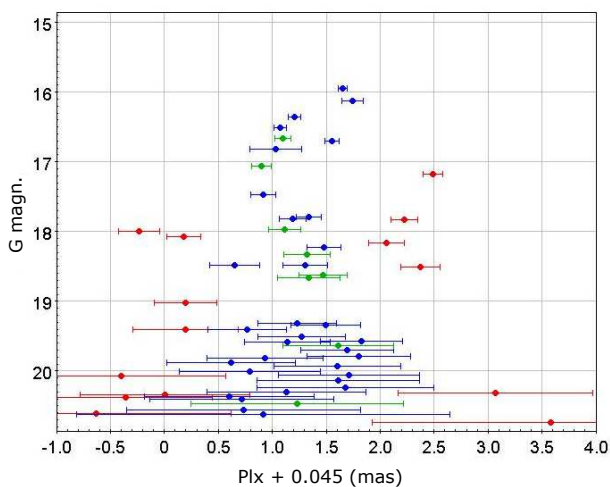
Finally, assuming that some of the nebulous stars in the investigated field belong to SL 4 dark cloud, we selected

Table 2. List of the probable members of BBWo 192E cluster

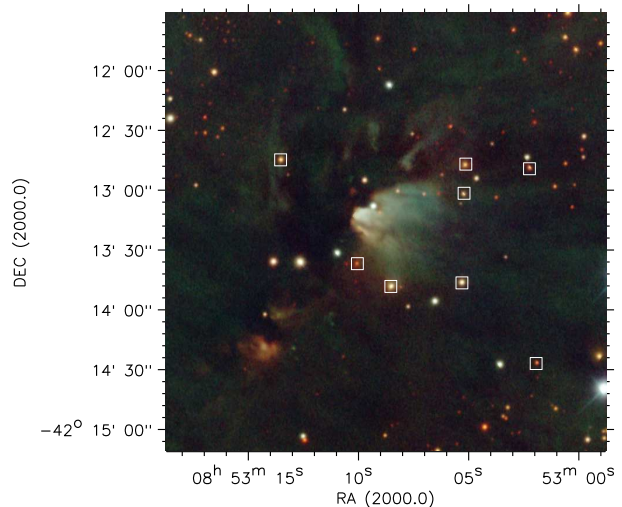
DR2Name	RA (ICRS), degr	Dec (ICRS), degr	Distance, pc		
			Most probable	Min	Max
Gaia DR2 5524333136802415232	133.24088919944	-42.24554393145	733	468	1573
Gaia DR2 5524356574444023168	133.27889063691	-42.23056943224	931	869	1005
Gaia DR2 5524356608803767680	133.26043332165	-42.22976576506	1143	1030	1283
Gaia DR2 5524356707582850176	133.30762774432	-42.20570767714	924	804	1084
Gaia DR2 5524356673223197440	133.28786696999	-42.22603423908	1493	674	3149
Gaia DR2 5524356845021802240	133.25994547813	-42.21249223335	791	667	970
Gaia DR2 5524356845021803392	133.25961283028	-42.20670598232	804	624	1124
Gaia DR2 5524356879381541632	133.24276963092	-42.20732210284	709	605	855

Table 3. Emission and nebulous stars probably related to SL 4 dark cloud

Gaia DR2 name	Other names	Nebula	Distance, pc		
			Most probable	Min	Max
5524522218442923520	ESO-H α 2348	BBWo 192C	865	839	893
5524545823586550400		BBWo 192D, GN 08.51.1.01	968	768	1301
5524519989361683840	ESO-H α 249	BBWo 192B, GN 08.50.5	1028	1004	1053
5524357742675055232	ESO-H α 260		958	876	1055
5524520019419933824	ESO-H α 248		962	880	1060


Figure 8. The correlation between visible magnitudes and parallaxes for all stars in BBWo 192E field, measured in GAIA DR2. The stars with parallaxes in 0.7–1.8 mas range are shown by blue, stars with similar PM – by green. All other stars in the field are marked with red color.

10 objects from the list of [Pettersson & Reipurth \(1994\)](#) and BBWo catalog. With the aid of Plx-Gmag and PM diagrams we excluded ESO-H α 244 as a foreground object and ESO-H α 255, 256 and 257 as background objects. ESO-H α 258 has large measurement errors. The remaining 5 stars are listed in Table 3 with their distances from the catalogue of [Bailer-Jones et al. \(2018\)](#). Their mean distance is 960 ± 50 pc, which confirms their belonging to SL 4 cloud. However, these nebulae and emission-line stars are slightly more distant than the probable member stars of the BBWo 192E cluster, located in the most opaque part of the cloud.


Figure 9. Eight stars with close PM and distances, which are the probable members of BBWo 192E cluster, are marked by white squares on the color image of the field, taken from DECaPS survey.

GAIA DR2 shows that our distance estimate of 800 ± 100 pc to the SL 4 cloud is lower than the previously estimated distance ([Burkert et al. 2000](#)). Our determined distance is similar to the 866 to 965 parsec distance of the Vela Complex ([Zucker et al. 2020](#)). For the further estimations of bolometric luminosities we use 800 pc value as based solely on the stellar parallaxes.

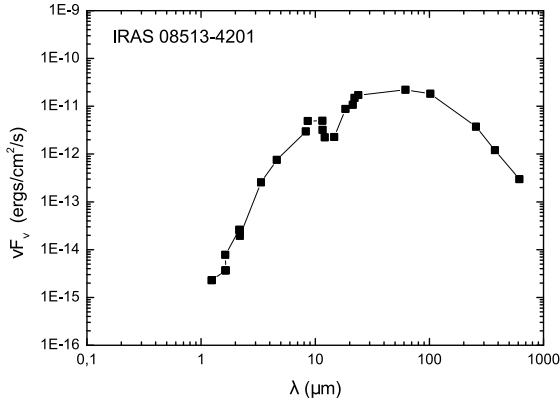


Figure 10. Spectral energy distribution (SED) of IRAS 08513–4201, based on the data, selected from literature.

4 DISCUSSION AND CONCLUSION

The most luminous infrared source in the BBW 192E cluster, IRAS 08513–4201 (also known as IRS 26-15), was analyzed in [Pettersson & Reipurth \(1994\)](#) and [Burkert et al. \(2000\)](#). It can be unambiguously identified with 2MASS 08530946–4213076 and WISE J085309.32–421397.3. The 2MASS point source catalog lists two more nearby sources (08530938–4213051 and 08530898–4213093), but the close inspection shows that they probably represent the brightest parts of the IR reflection nebula. We added photometry from the MSX6C catalog ([Egan et al. 2003](#)), the AKARI/IRC mid-infrared all-sky survey, and sub-mm observations using the BLAST telescope ([Netterfield et al. 2009](#)) to build the spectral energy distributions (SED) for this object. The SED of IRAS 08513–4201 is shown in Fig. 10. The SED is broad, suggesting a wide range of dust temperatures. We estimate bolometric luminosity of IRAS 08513–4201 to be $L \approx 1010 L_{\odot}$, slightly lower than previous estimates because of the smaller adopted distance. This object is likely to be an intermediate-mass HAeBe star.

Fig. 11 shows the SEDs of other IR sources, described in Sec. 3.2. These SEDs use photometry from 2MASS and allWISE since they were not detected in longer wavelength surveys. All of these objects emit at wavelengths longer than $2 \mu\text{m}$ which demonstrates high foreground extinction. We estimated lower-bounds on their luminosities by integrating the SEDs over the observed range. Their luminosities range from $L > 0.5$ to $2.9 L_{\odot}$. Since no far-IR data exist, we computed the bolometric corrections using the approach suggested by [Cohen \(1973\)](#). The corrected bolometric luminosities of these 5 sources range from 2 to $6 L_{\odot}$ with J085309.91-421232.6 (IRS 26-35) being the most luminous. Thus, these are typical T Tauri class stars. Thus, the SL 4 cloud contains a small group of forming and young low mass stars surrounding a more massive HAeBe star.

An interesting feature of the SL 4 cloud is the absence of any HH flows connected to IRAS 08513–4201, the most luminous source. On the other hand, the existence of the optical HH flows around both the reflection nebulae and the cluster of YSOs suggests that star formation in this cloud

is on-going. Assuming a typical flow velocity of 100 km s^{-1} and a characteristic separation of the HH objects from likely sources, their kinematic ages cannot be more than several thousand years. The presence of some YSOs and ionized flows in the visual wavelength images indicates that some members of this group of young stars are not heavily embedded in the dark cloud, and the significant part of line-sight extinction can be produced in the dusty circumstellar disks and envelopes.

The SL 4 star-forming region is similar to the zone of star formation near CPM 19 ([Khanzadyan et al. 2011](#), and references therein). SL 4 may be an interesting target for the study shock-excited H_2 emission. Multi-epoch monitoring would be useful for the identification of erratic variables and occasional multi-magnitude accretion-powered flares. Unfortunately, this field was not observed by either the Spitzer or Herschel surveys. If the BBW 192E nebula is illuminated by IRAS 08513–4201, then its visual wavelength or near-IR spectrum could be obtained by observing the reflection nebula it produces. Such a study could provide further insights into the mass and evolutionary state of this embedded object. Finally, given its southern location, the BBW 192E star forming region is ideally placed for deep millimeter and sub-millimeter-wave studies with ALMA.

ACKNOWLEDGEMENTS

Authors thank Prof. B.Reipurth for providing the numbers of new HH objects. This work was supported by the RA MES State Committee of Science, in the frames of the research projects number 15T-1C176 and 18T-1C-329. A.S. Rastorguev also acknowledges RFBR grants Nos. 18-02-00890, 19-02-00611 for partial financial support. This research has made with constant use of “Aladin sky atlas” and other products developed at CDS, Strasbourg Observatory, France. This publication makes use of data products from the Two Micron All Sky Survey, which is a joint project of the University of Massachusetts and the Infrared Processing and Analysis Center/California Institute of Technology, funded by the National Aeronautics and Space Administration and the National Science Foundation. This publication makes use of data products from the Wide-field Infrared Survey Explorer, which is a joint project of the University of California, Los Angeles, and the Jet Propulsion Laboratory/California Institute of Technology, funded by the National Aeronautics and Space Administration. This publication has made use of data from the European Space Agency (ESA) mission *Gaia* (<https://www.cosmos.esa.int/gaia>), processed by the *Gaia* Data Processing and Analysis Consortium (DPAC, <https://www.cosmos.esa.int/web/gaia/dpac/consortium>). Funding for the DPAC has been provided by national institutions, in particular the institutions participating in the *Gaia* Multilateral Agreement.

DATA AVAILABILITY

The data underlying this article will be shared on reasonable request to the corresponding author.

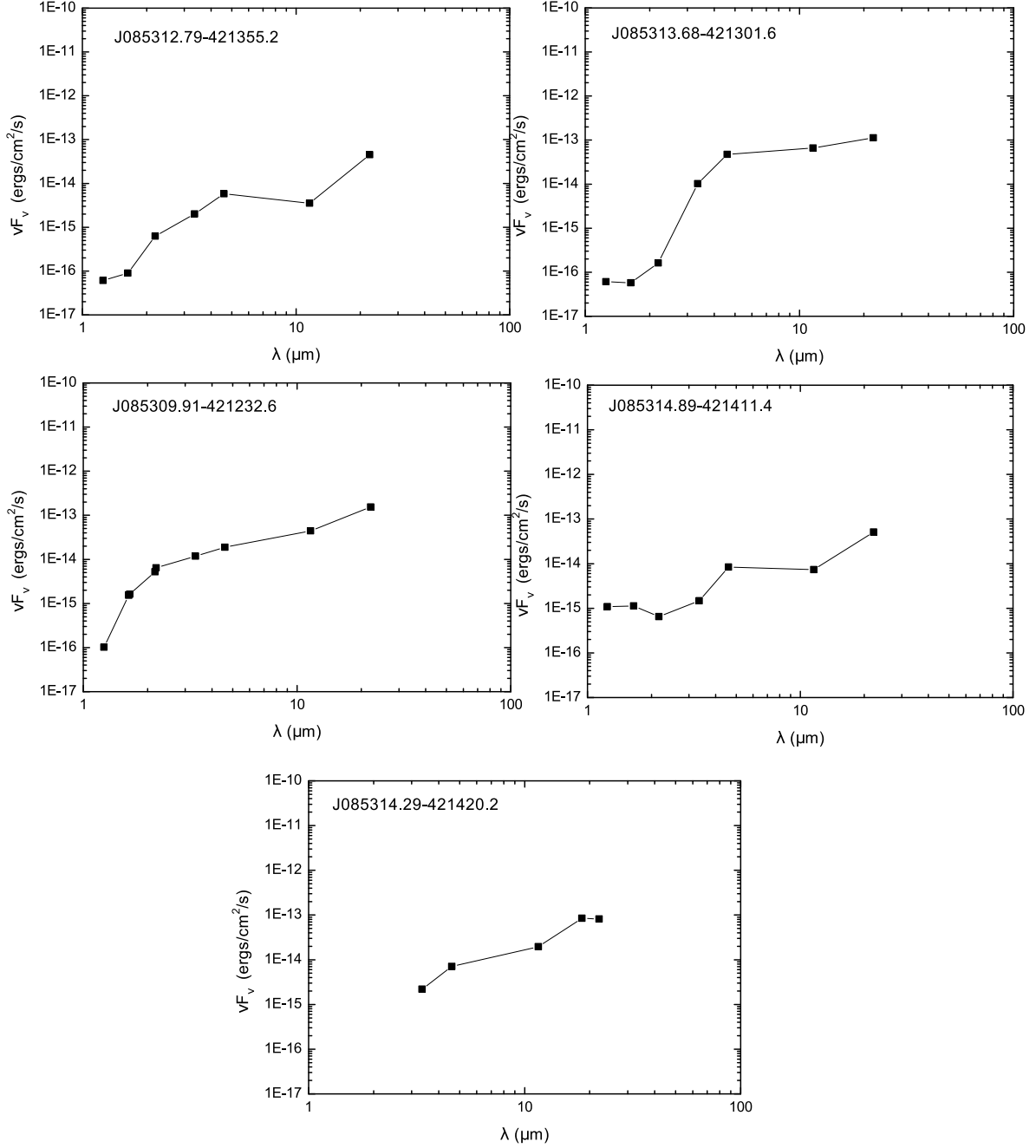


Figure 11. SEDs of other IR sources in the vicinity of IRAS 08513–4201.

REFERENCES

- Bailer-Jones, C.A.L., Rybizki, J., Fouesneau, M., Mantelet, G., & Andrae, R. 2018, *AJ*, 156, id.58
- Burkert, A., Stecklum, B., Henning, T. & Fischer, O. 2000, *A&A*, 353, 153
- Brand J., Blitz L., & Wouterloot J.G.A., 1986, *A&A*, 65, 537
- Cohen, M. 1973, *MNRAS*, 164, 395
- Dutra, C.M., Bica, E., Soares, J & Barbuy, B. 2003, *A&A*, 400, 533
- Egan M.P., Price S.D., Kraemer K.E., et al., 2003, *VizieR Online Data Catalog*, V/114
- Gyulbudaghian A.L., Magakian T.Yu., 1977, *Lett. to AZh*, 3, 113
- Ishihara D., Onaka T., Kataza H., et al., 2010, *A&A*, 514, A1
- Khanzadyan T., Movsessian T.A., Davis C.J. et al. 2011, *MNRAS*, 418, 1994
- Liseau R., Lorenzetti D., Nisini B. et al. 1992, *A&A*, 265, 577
- Massi, F., Lorenzetti, D. & Giannini, T. 2003, *A&A*, 399, 147
- Murphy, D. & May, J. 1991, *A&A*, 247, 202
- Netterfield, C.B., Ade, P.A.R., Bock, J.J. et al. 2009, *ApJ*, 707, 1824
- Petterson, B. & Reipurth, B. 1994, *A&AS*, 104, 233
- Sandqvist, A. & Lindroos, K. 1976, *A&A*, 53, 179

- Schlafly, E.F., Green, G.M., Lang, D. et al. 2018, ApJS, 234, 39
Schönrich, R., McMillan, P., & Eyer, L. 2019, MNRAS, 487, 3568
Wright, E.L., Eisenhardt, P.R.M., Mainzer, A.K. 2010, AJ, 140, 1868
Zucker, C., Speagle, J.S., Schlafly, E.F. et al. 2020, A&A, 633, A51